Q. J. R. Meteorol. Soc. (1998), **999**, pp. 1–22

The Dependence of clear-sky Outgoing Longwave Radiation on Surface Temperature and Relative Humidity

By R. P. ALLAN[1]*, K. P. SHINE[1], A. SLINGO[2] and J. A. PAMMENT[2]

[1] *University of Reading, UK*
[2] *Hadley Centre, Meteorological Office, UK*

(Received January 1998; revised August 1998)

Summary

A simulation of the Earth's clear-sky longwave radiation budget is used to examine the dependence of clear-sky outgoing longwave radiation (OLR) on surface temperature and relative humidity. The simulation uses global ECMWF reanalysed fields to calculate clear-sky OLR over the period from January 1979 to December 1993, thus allowing the seasonal and interannual time-scales to be resolved. The clear-sky OLR is shown to be primarily dependent on temperature changes at high latitudes and on changes in relative humidity at lower latitudes. Regions exhibiting a super-greenhouse effect are identified and are explained by considering the changes in the convective regime associated with the Hadley circulation over the seasonal cycle, and the Walker circulation over the interannual time-scale. The sensitivity of clear-sky OLR to changes in relative humidity diminishes with increasing relative humidity. This is explained by the increasing saturation of the water vapour absorption bands with increased moisture. By allowing relative humidity to vary in specified vertical slabs of the troposphere over an interannual time-scale it is shown that changes in humidity in the mid-troposphere (400 to 700 hPa) are of most importance in explaining clear-sky OLR variations. Relative humidity variations do not appear to affect the positive thermodynamic water vapour feedback significantly, in response to surface temperature change.

Keywords: Clear-sky longwave radiation Water vapour feedback Super-greenhouse effect

1. INTRODUCTION

Outgoing longwave radiation to space, OLR, is the fundamental cooling mechanism of the Earth-atmosphere system. Knowledge of its dependence on surface and atmospheric parameters is therefore required for a quantitative understanding of the climate and climate change. The response of the climate system to a change in the Earth's radiation budget is made more complex by feedbacks, one of which involves a change in water vapour amount and distribution in response to a change in surface temperature, T_s. Water vapour is generally regarded to provide a positive feedback with climate models implying an amplification of surface warming of about 1.6 (e.g. IPCC 1990).

Raval and Ramanathan (1989) used satellite Earth Radiation Budget Experiment (ERBE) observations of clear-sky OLR to argue in favour of a positive water vapour feedback, by showing an increase in normalised atmospheric greenhouse trapping with spatially increasing T_s. However, spatial variations cannot be used reliably to infer water vapour changes in a warming climate; Spencer and Braswell (1997) noted that a positive feedback will always apply spatially between the ascending and descending branches of the tropical circulation systems. Rind *et al.* (1991) showed satellite-derived water vapour amounts to increase with the greater convection associated with hemispheric warming over the seasonal cycle. They concluded that the quantitative agreement with climate model predictions strengthens the argument in favour of a positive water vapour feedback. Ramanathan and Collins (1991) inferred a positive feedback spatially and over short time-scales such as the seasonal cycle and the El Niño/Southern Oscillation (ENSO). However, Lau *et al.* (1996) pointed out that it is not prudent to assume that feedbacks operating

* Corresponding author: Department of Meteorology, University of Reading, Earley Gate, PO BOX 243, Reading, Berkshire, RG6 6BB, UK. E-mail: r.p.allan@rdg.ac.uk

over these time-scales are relevant for climate change on decadal time-scales unless entire circulation systems are accounted for.

Bony *et al.* (1995) calculated the sensitivity of ERBE clear-sky OLR to T_s using the monthly-means of 1987 and 1988. The difference between the sensitivity of the clear-sky OLR to T_s over different time-scales and between the ERBE and climate model warming experiments was attributed to changes in temperature lapse rate and relative humidity, RH. Raval *et al.* (1994) also highlighted the strong seasonal correlation between ERBE OLR and column mean RH for both clear and cloudy skies over the tropical oceans. The relationship between upper tropospheric RH (UTH), deep convection frequency and the normalised clear-sky atmospheric greenhouse trapping was examined by Soden and Fu (1995). From the correlation, they inferred that variations in UTH explain about half of the deviation of normalised greenhouse trapping from its climatological mean, with the remainder being tentatively explained by variations in the temperature lapse rate and moisture at lower levels. Sinha and Harries (1997) concluded that while clear-sky OLR is most sensitive to upper tropospheric RH, changes in RH in the middle troposphere are largest. The prime motivation of the present study is to extend this earlier work by using a simulation of clear-sky OLR based on 15 years of data. The longer period of analyses, than earlier studies, allows a more robust characterisation of the variability; and the use of a model to simulate the OLR allows the causes of the variability to be more clearly identified than is possible using statistical analyses, where relationships between variables may not adequately imply a direct causal link.

Another focus for this study is to examine the occurrence of the super-greenhouse effect (SGE) (e.g. Hallberg and Inamdar 1993) which describes the apparently unstable clear-sky longwave radiative feedback operating at high sea surface temperatures whereby clear-sky OLR is anti-correlated with T_s. An additional feedback must be present to stabilise tropical sea surface temperatures; suggested mechanisms are shortwave cloud radiative forcing (Ramanathan and Collins 1991), evaporative feedbacks (Hartmann and Michelsen 1993) and heat export to the extra tropics (Pierrehumbert 1995). Bony *et al.* (1997) explained the SGE occurrence by considering the changes in convective regime associated with the large-scale circulation over the seasonal and interannual time-scale.

The present study uses a simulation of the Earth's clear-sky longwave radiation budget, described in section 2, to assess the impact of changes in temperature and humidity throughout the atmosphere on clear-sky OLR. Slingo *et al* (1998) showed the quality of the simulation by comparing clear-sky OLR with that from ERBE. The present study benefits from a sufficiently long data set to allow climate fluctuations on a longer time-scale than the ERBE period to be resolved, and includes several ENSO events. Land and oceans are sampled, thus ensuring global coverage of clear-sky irradiance and sampling of the entire atmospheric circulation system. Thus the sensitivity of clear-sky OLR to surface and atmospheric parameters may be calculated in a global-mean sense. The framework of interpretation of the present analysis is set out in section 3 while results are described in sections 4 and 5. Discussion with reference to the super-greenhouse effect and the water vapour feedback are presented in the final section.

2. SIMULATION

A comprehensive re-analysis of atmospheric variables for a 15-year period was performed by the European Centre for Medium-Range Weather Forecasts Re-Analysis project (ERA). Slingo *et al.* (1998) used the ERA analyses to perform simulations of clear-sky longwave fluxes and heating rates, with the acronym CLERA (Clear-sky Longwave from ERA). Radiative calculations were performed with the 9 spectral band version of the Edwards and Slingo (1996) radiation code for every 6 hours from January 1979 to December 1993. Surface emissivity was set to unity for consistency with the ERA model. The ERA data was used on a 2.5° by 2.5° horizontal grid, with 31 sigma levels in the vertical in the atmosphere and also the surface temperature. The well-mixed greenhouse gas concentrations (CO_2, CH_4, N_2O, CFC11, CFC12) were updated annually in accordance with IPCC (1995). Ozone was derived from a monthly-mean climatology (Cullen 1993) and was assumed to be fixed throughout the analysis period. Interannual variations in ozone are unlikely to affect the OLR variability significantly. Clear-sky profiles were assumed throughout, even in cloudy regions, thus ensuring that information on clear-sky irradiance was sampled globally. The definition is consistent with the way in which clear-sky fluxes are calculated in climate models, but it differs from that used by ERBE studies which only class regions as clear-sky if the statistical likelihood of cloud is sufficiently low. Studies using ERBE data are thus prone to cloud contamination of clear-sky regions (e.g. Slingo and Webb 1992) and a tendency towards the sampling of drier profiles. The present study used monthly-means of the simulated clear-sky OLR together with the ERA data. Further experiments were performed with the CLERA simulation using mean profiles for the Julys in each of the 15 years, in which water vapour amounts are perturbed to assess the role of RH throughout the troposphere in influencing clear-sky OLR variability.

Unique to the CLERA system are the length and time resolution of the data set and its global coverage (land and ocean). Because ERA combines a wide range of atmospheric and surface data using the same analysis system throughout the data period, it constitutes one of the most robust representations of global conditions and variability over a 15 year period, including that of RH. However, because most relevant RH data is assimilated, independent validation of this parameter is problematic. The CLERA simulation calculates RH with respect to water. A more accurate definition is not required because RH is used in this study as a diagnostic parameter, rather than as a prognostic variable to determine the degree of saturation of water vapour in the atmosphere. Errors in ERA T_s and surface emissivity, while affecting the absolute calculation of clear-sky OLR, are unlikely to be significant with regard to monthly-mean variability.

3. FRAMEWORK

To assess the dependence of clear-sky OLR on atmospheric structure it is useful to examine the radiative transfer equation. Outgoing longwave radiation to space for clear-sky conditions may be expressed as:

$$OLR = \int_{v=0}^{v=\infty} \left[(B_v(0) Tr_v(p_s, 0)) + \int_{p_s}^{0} B_v(p) \frac{dTr_v(p,0)}{dp} dp \right] dv, \tag{1}$$

where $B_v(p)$ denotes the black body emission at pressure, p, and $Tr_v(p_s, 0)$ denotes the transmittance between the surface pressure, p_s, and the top of the atmosphere. The subscript v denotes wavenumber and both B and Tr include implicit integration over the zenith angle to convert radiance to irradiance. Equation 1 may be simplified to,

$$OLR = \sigma {T_s}^4 Tr + OLR_a(T(p), q(p)), \tag{2}$$

where $\sigma {T_s}^4$ is the wavelength integrated (black body) surface emission and Tr is the *effective* atmospheric transmittance. It is an effective transmittance because the transmission varies with wavelength and therefore the Planck function becomes more important in the relatively transparent window regions of the spectrum. The second right hand term represents the atmospheric emission which is dependent primarily on temperature, T, and specific humidity, q, throughout the profiles as well as the concentration of CO_2 and other greenhouse gases.

Increasing atmospheric T in Eq. (2) acts to increase the longwave emission to space from the atmosphere, while increases in q act to decrease the surface component of the OLR and also decrease OLR$_a$ by shifting emission to a higher, generally colder layer. Thus it is useful to explain the clear-sky OLR in terms of surface and atmospheric temperature and water vapour amounts. Shine and Sinha (1991) show that clear-sky OLR is sensitive to relative changes in q throughout the atmosphere but that clear-sky OLR is far more sensitive to absolute changes in q in the upper troposphere than at other levels. Therefore, in developing an atmospheric humidity parameter that describes adequately the clear-sky OLR variability, it is more useful to consider the RH rather than the total column moisture. A further reason for using RH is that T and q have opposing effects on the clear-sky OLR, which almost cancel in the water vapour bands if relative humidity is held constant (Slingo and Webb 1997). However, the cancellation is not complete because water vapour does not absorb strongly over the entire spectrum. Because atmospheric temperature, T_a, is coupled to a certain degree with T_s, a change in clear-sky OLR may be expressed as a function of a change in T_s and a change in tropospheric relative humidity, TRH:

$$\Delta OLR = \left[4\sigma T_s^3 \overline{Tr} + \left(\sigma T_s^4 \frac{\partial Tr}{\partial T_a} + \frac{\partial OLR_a}{\partial T_a} \right)_{(\overline{RH})} \frac{dT_a}{dT_s} \right] \Delta T_s$$

$$+ \left(\sigma T_s^4 \frac{\partial Tr}{\partial TRH} + \frac{\partial OLR_a}{\partial TRH} \right) \Delta TRH, \tag{3}$$

from which it follows that,

$$\Delta OLR = (4\sigma {T_s}^3 \overline{Tr} + \alpha)\Delta T_s + \frac{\partial OLR}{\partial TRH} \Delta TRH. \tag{4}$$

The TRH used here is defined in section 4(b), but approximates as the column average relative humidity between about 100 and 900 hPa with maximum weight at $450 hPa$. Equation (4) shows that there is dependence of OLR variability on T_s and TRH and is a similar model to that developed by Thompson and Warren (1982). The parameter, α ($Wm^{-2}K^{-1}$), denotes an amplification of clear-sky OLR response to ΔT_s by changes in atmospheric temperature with constant RH.

The analysis framework used to infer sensitivities and correlation is that of linear least squares fit (LSQF) (e.g. Freund 1976). This removes the potential for misinterpretation by considering only particular months as pointed out by Soden (1997). The sensitivity and the degree of linear correlation of clear-sky OLR to T_s and TRH may be calculated over the 12 month seasonal cycle of a particular year, and the 15 year interannual time-scale for a particular month. This differs from the technique used by Bony *et al.* (1995, 1997) who calculate a *spatial* correlation between sea surface temperature and ERBE clear-sky OLR differences between seasons and between years for all grid points in a particular temperature bin. A correlation coefficient, r, of greater than 0.75 or less than -0.75 is required for a significant correlation at the 99.5% significance level for the smallest sample size used here (12 months).

4. REGRESSION STUDIES

(a) *Surface Temperature*

Figure 1(a) shows the LSQF regression correlation for clear-sky OLR and T_s calculated over the seasonal cycle for 1985. There is a strong positive correlation between clear-sky OLR and T_s for latitudes pole-wards of about $\pm 30°$. In the tropics the correlation tends to be negative, showing that changes in atmospheric structure act to counteract the direct ΔT_s contribution to changing clear-sky OLR in Eq. (4). In these regions, simulated clear-sky OLR decreases with increasing T_s, constituting a potentially unstable feedback. This has been termed the super-greenhouse effect (SGE) (e.g. Ramanathan and Collins 1991). Over high latitude oceans, changes in atmospheric temperature act to amplify the sensitivity of clear-sky OLR to T_s (Webb *et al.* 1993); clear-sky OLR changes are greater than changes in surface emission due to large increases in OLR_a with increased T_s. In this situation the parameter, α in Eq. (4), is large because atmospheric temperatures are changing at a greater rate than T_s. The relationship between clear-sky OLR and T_s over the seasonal cycle of other years is similar to that of 1985.

Over the interannual time-scale for July (Fig. 1(b)) a SGE at high T_s is still present. These regions are confined to the tropical oceans and are less coherent than for the seasonal cycle. Strong positive correlation is confined mainly to land areas of latitude greater than about 45° where changes in T_s are greatest and convection strongly couples T_a and T_s thus increasing α. The simulated sensitivities are between about 1 and 3 $Wm^{-2}K^{-1}$ away from the tropical oceans and are negative over the tropical oceans; this is consistent with Bony *et al* (1995) who use ERBE data from 1987 to 1989 and a climate model applied to seasonal and interannual time-scales. Applying the LSQF analysis to interannual time-scales for months other than July results in similar sensitivities of clear-sky OLR to T_s, although regions exhibiting a SGE vary in latitude.

The regions exhibiting a SGE are consistent with the results of Bony *et al.* (1997) who use ERBE clear-sky OLR from 1985 to 1989 and may be explained by considering the changes in the large scale circulation. Over the seasonal cycle (Fig. 1(a)), regions exhibiting a SGE are generally situated within the 5 to 15° latitudinal zones either side of the equator. The change in convective regime related to the north-south shift of the Hadley Cell over the seasonal cycle is larger in these regions than at the equator and forces large changes in TRH which decouple the clear-sky OLR from surface emission. Over the interannual time-scale, the shift in the Hadley circulation is small, although a residual SGE signal is present over the Atlantic and Indian oceans. The strongest SGE signal is evident in the tropical central Pacific, due to shifts in the Walker circulation associated with ENSO events.

(b) *Tropospheric Relative Humidity*

Increasing RH acts to decrease the surface component of the clear-sky OLR by decreasing Tr in Eq. (2) and effectively shifts the height of atmospheric longwave emission to space up to a colder level thus decreasing OLR_a. As absorption bands are radiatively

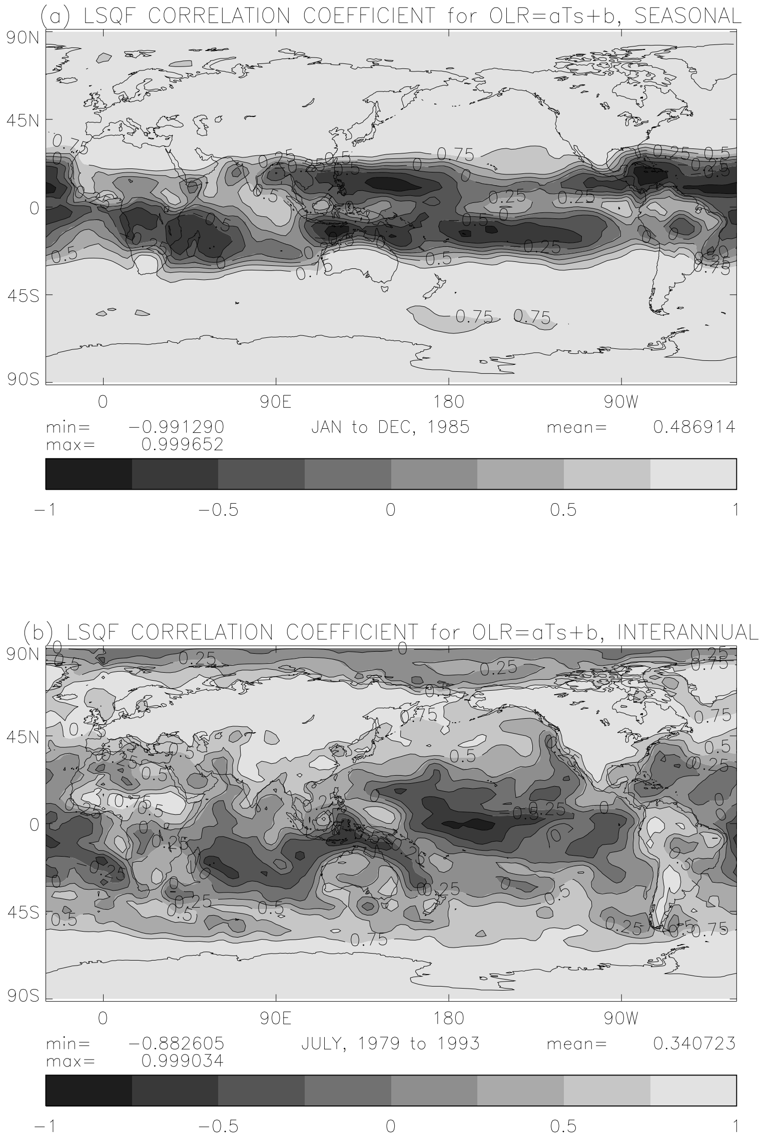

Figure 1. LSQF correlation coefficient for $OLR = aT_s + b$ using the CLERA simulation over (a) the seasonal cycle for 1985 and (b) the interannual time-scale for July. The contour interval is 0.25.

less saturated with decreasing q, the sensitivity of the clear-sky OLR to RH is most negative for drier profiles and also for changes in RH in the relatively dry upper troposphere. This is complicated by the absorption properties of the water vapour continuum (e.g. Clough *et al.* 1992) which, in the moister profiles, acts to decrease the surface component of the clear-sky OLR with increased RH in the lower troposphere.

To illustrate this point a narrow band radiative transfer scheme (Forster and Shine 1997) was applied to a tropical standard profile (McClatchey *et al* 1972) which has RH set to 40% between 100 and 1000 hPa. The changes in OLR are plotted as a function of wavenumber in Fig. 2 for specified uniform changes in RH between 100 and 1000 hPa.

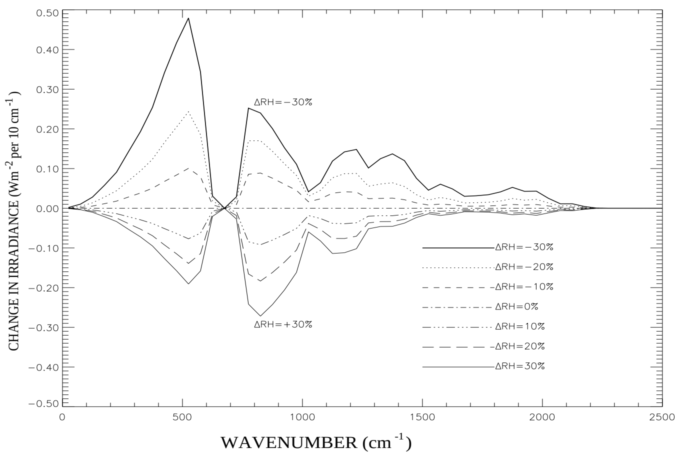

Figure 2. Narrow band model calculated spectral changes in clear-sky OLR as a function of wavenumber (cm^{-1}) with uniform RH changes between 100 and 1000 hPa for a tropical standard profile with the RH set initially at 40%.

In the major water vapour bands (approximately wavenumbers less than 600 cm^{-1} and greater than 1200 cm^{-1}), absolute changes in OLR are greater for a given decrease in RH than for the same magnitude *increase* in RH confirming the non-linear increase in OLR with decreasing RH. In the window region of the spectrum (approximately 800 to 1200 cm^{-1}) there is an approximately linear negative dependence of clear-sky OLR on RH. The water vapour bands vary in their degree of saturation, so the altitude of maximum contribution to OLR varies throughout the upper and middle troposphere (i.e. about 100 to 800 hPa) depending on wavenumber. Because continuum absorption in the window region mainly acts in the lower troposphere (i.e. pressures greater than about 600 hPa), RH variations throughout the atmosphere are significant in determining clear-sky OLR. This is consistent with the findings of Shine and Sinha (1991).

Considering Eq. (4), a TRH parameter that adequately describes variations in clear-sky OLR must account for the changes in RH in the regions of the atmosphere that are most important in determining clear-sky OLR variability. The dependence of clear-sky OLR on changes of RH ($\Delta OLR_{\Delta RH}$) may be written as a function of its sensitivity to RH at pressure, p, and the change in $RH(p)$:

$$\Delta OLR_{\Delta RH} = \frac{\partial OLR}{\partial RH(p)} \Delta RH(p). \tag{5}$$

Figure 3(a) characterises the ERA RH variability by calculating its standard deviation, SD (%), at each sigma level for the monthly-means of July (1979 to 1993) between 40°N and 40°S (solid line). The $\partial OLR/\partial RH(p)$ term is provided by the narrow band scheme applied to a tropical standard atmosphere for 1% increases in RH (Fig. 3(b)). While clear-sky OLR is most sensitive to RH in the upper troposphere (about 250 hPa), variations in ERA RH are greatest in the middle and lower troposphere (about 600 to 800 hPa). Therefore the inferred OLR variation due to ERA $\Delta RH(p)$, from Eq. (5), is greatest between about 200 to 850 hPa with contribution from the entire troposphere (Fig. 3(c), solid line). The calculated OLR variation assumes that ERA provides a good representation of the true RH variability. In reality, there is significant uncertainty attached to the humidity throughout the atmosphere, especially at higher altitudes (e.g. McNally and Vesperini (1996)). Therefore estimates of RH interannual variability must be received with caution. A further calculation was performed whereby RH standard deviation was assumed to increase linearly from 5% at 1000 hPa to 15% at the top of the atmosphere (Fig. 3(a), dotted line). This 'high variability scenario' (HVS) assumes ERA humidity variability to be underestimated with the largest underestimation at high altitudes. By calculating the resulting OLR variability (dotted line, Fig. 3(c)), the potential impact of the uncertainty in RH variability at higher altitudes is illustrated. The maximum OLR variability is due to RH variations is at about 250 hPa, but with significant contribution to the OLR variability from RH variations at lower altitudes. It is seen that the upper troposphere has the *potential* to affect the clear-sky OLR variability to a greater extent than lower levels if ERA humidity variation in the upper troposphere is underestimated. This caveat should be considered when using the ERA humidity in studies such as the present one and thus highlights the need for further work in addressing this uncertainty.

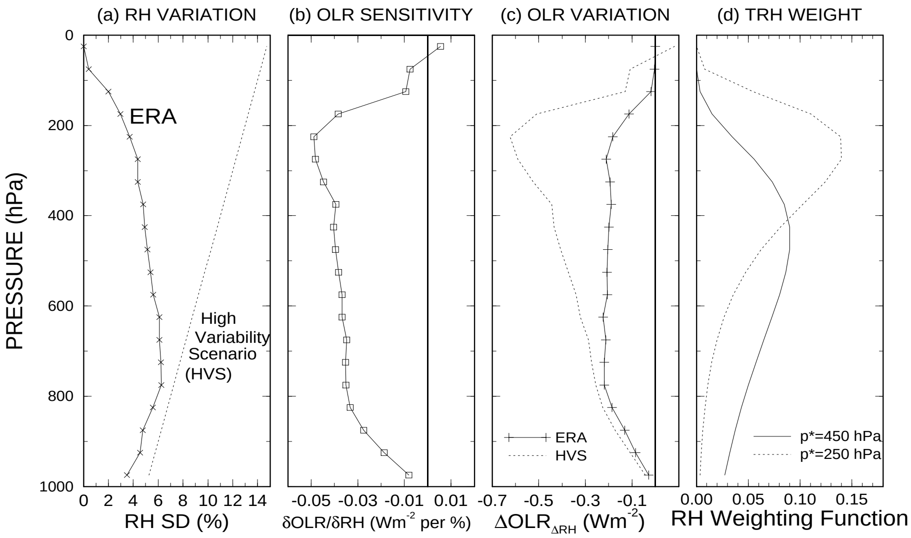

Figure 3. The importance of height dependent RH variations on clear-sky OLR variability: (a) 40°S to 40°N mean ERA RH Standard Deviation with pressure for the 15 monthly-mean July's of the ERA period (solid line) and a 'high variability scenario' (HVS) RH standard deviation (dotted line), (b) Narrow band calculated sensitivity of clear-sky OLR to height dependent 50 hPa slab changes in RH for the tropical standard atmosphere, (c) Inferred variation of clear-sky OLR due to ERA RH variations (solid line) and for the HVS RH variations (dotted line). (d) Weighting function applied to RH for evenly spaced 50hPa vertical slabs that is used to calculate TRH for p^*=450 hPa and p^*=250 hPa (Eq. (6)).

Soden and Fu (1995) use satellite retrievals of UTH (approximately 200 to 500 hPa RH) to show that the clear-sky normalised atmospheric greenhouse effect is strongly correlated with upper tropospheric RH, although they note that the lapse rate and lower tropospheric moisture may explain about half of this dependence. CLERA monthly-mean clear-sky OLR also shows a strong negative correlation with upper tropospheric RH in the tropics (not shown). Considering the importance of RH variations over the entire troposphere shown in Fig. 3, some of the correlation between upper tropospheric RH and clear-sky OLR may be due to a coupling between RH in the upper troposphere and RH at lower altitudes.

Taking the results of Fig. 3 into account, the parameter TRH is defined to account for RH throughout the troposphere, but to apply maximum weight to the middle troposphere:

$$TRH = \frac{\sum_{i=1}^{31} exp(-2(ln(p_i) - ln(p^*))^2) RH(p_i) \Delta p_i}{\sum_{i=1}^{31} exp(-2(ln(p_i) - ln(p^*))^2) \Delta p_i}, \tag{6}$$

where i denotes sigma level and p^* is the pressure at which maximum weight is prescribed to RH. The weighting function is plotted in Fig. 3(d) for evenly spaced 50 hPa thick slabs for p^*=450 hPa and p^*=250 hPa. A Gaussian form is chosen so as not to exclude entirely the RH variations in the regions of the atmosphere less important to the determination of clear-sky OLR. This is also more consistent with the form of the satellite derived upper tropospheric RH weighting function used by Soden and Fu (1995) than taking a column mean RH. It was decided to calculate TRH using p^*=450 hPa so as not to exclude the contribution of RH variation in the lower troposphere to changes in clear-sky OLR variability. Although there is significant uncertainty with regard to RH variability in the upper troposphere and stratosphere, the low weight prescribed to pressures less than 150 hPa is still valid given that clear-sky OLR is relatively insensitive to changes in RH at these levels (Fig. 3(b)). The calculated mean July TRH from 1979 to 1993 is plotted in Fig. 4. The dry descending regions of the sub-tropics are highlighted by TRH of below about 30%, while the ascending regions of the tropical warm pool and the Asian Monsoon as well as over central Africa are characterised by high TRH of above 60%.

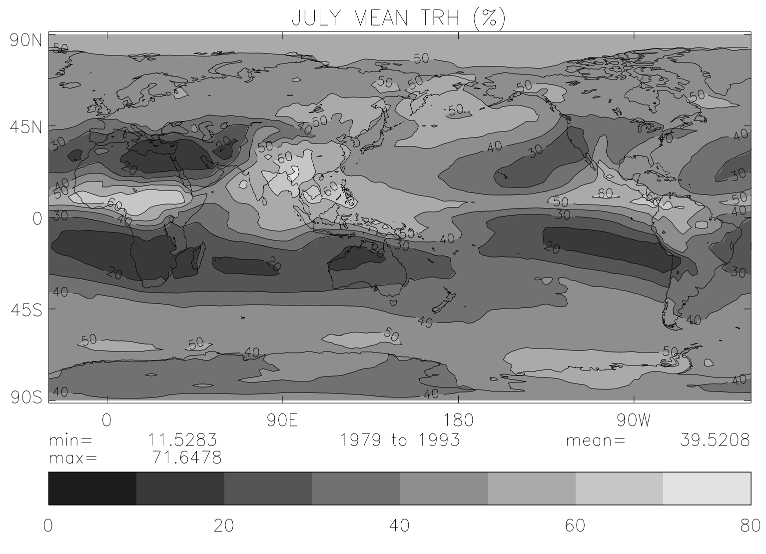

Figure 4. Calculated July mean TRH (%) for the ERA period. The contour interval is 10%.

Figure 5(a) shows that there is a strong negative correlation between clear-sky OLR and TRH over the seasonal cycle of 1985 within about 30° of the equator. Away from the tropics, the correlation is smaller and tends to be positive which implies that changes in other parameters are influencing clear-sky OLR changes. The region of strong negative correlation over the interannual time-scale for July extends up to 45° away from the equator and the global average correlation coefficient is -0.7 (Fig. 5(b)). TRH explains more of the variance in OLR over the interannual time-scale than over the seasonal cycle because temperature fluctuations are smaller from year to year than over a season. The correlation distribution is similar when setting p^* to 250 hPa (not shown). Comparing Fig. 5 and Fig. 1 it is apparent that TRH explains most of the clear-sky OLR variations at low latitudes while T_s is important in explaining clear-sky OLR variations at high latitudes.

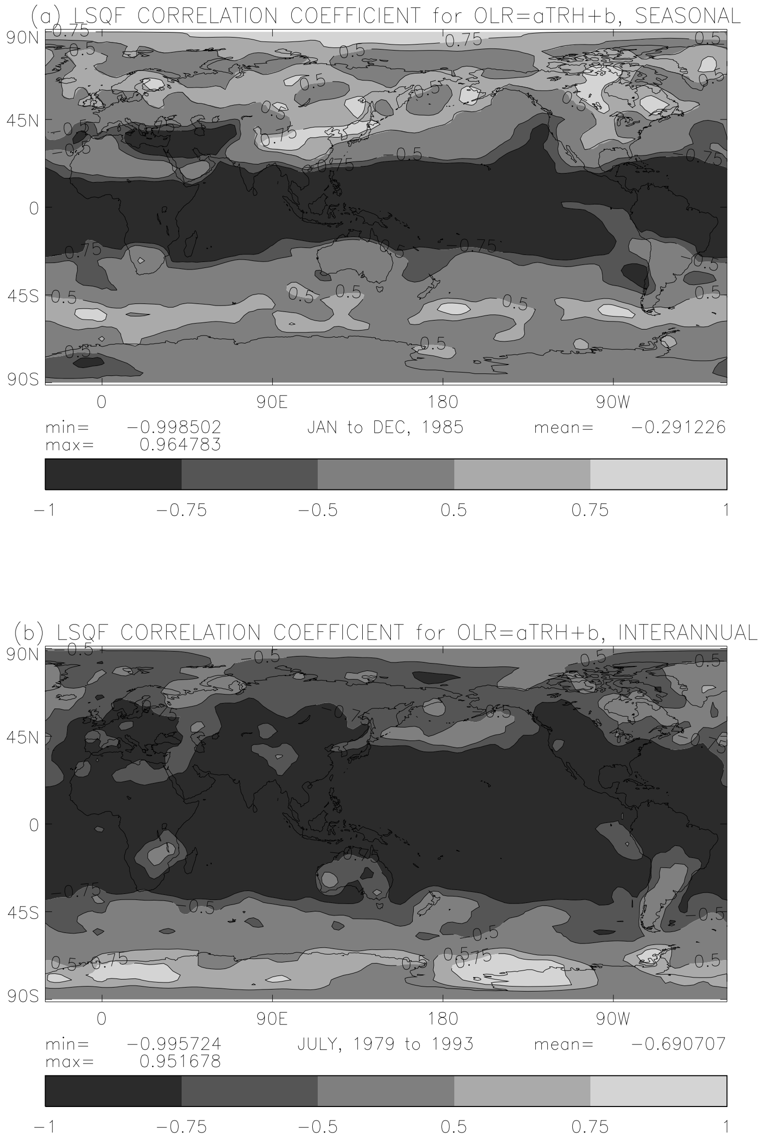

Figure 5. LSQF correlation coefficient for $OLR = aTRH + b$ from CLERA over (a) the seasonal cycle of 1985 and (b) for July over the ERA period.

Figure 6 shows the July LSQF clear-sky OLR sensitivity to TRH ($dOLR/dTRH$) with mean TRH for grid points where correlation is significant at the 99.5% significance level. The corresponding values calculated by the narrow band scheme when RH is varied between 100 and 1000 hPa in the tropical standard profile are also plotted (solid line).

The scatter of points about the narrow band calculated sensitivity are likely to be the result of OLR sensitivity to temperature variations as described in Eq. (4). The TRH parameter also cannot capture the changes in RH throughout the atmosphere, introducing an additional source of error. Nevertheless, the simulation captures the tendency for $dOLR/dTRH$ to be most negative in the regions with the lowest mean TRH because the water vapour absorption bands are saturating with increasing RH (Fig. 2). The increased sensitivity of clear-sky OLR to TRH for the drier descending regions of low TRH highlighted in Fig. 4 are important with regard to the water vapour feedback for two further reasons: (a) The dry descending regions contain a high proportion of clear-skies and cover large areas of the tropics and, (b) radiative processes in these regions significantly affect the total heating.

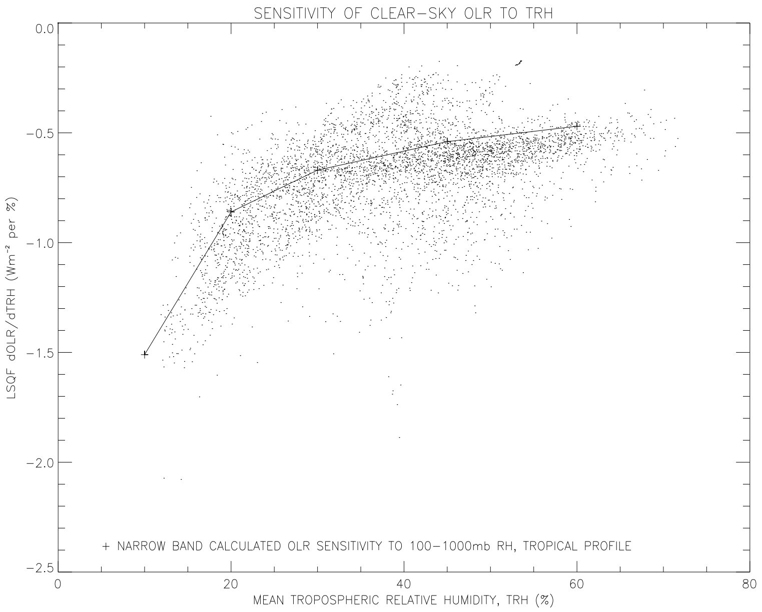

Figure 6. LSQF sensitivity of clear-sky OLR calculated by CLERA to changes in TRH (Wm^{-2} per %) with mean TRH for July, 1979 to 1993. Only grid points of significant correlation above the 99.5 % level are plotted. The solid line denotes the corresponding narrow band calculated sensitivities when RH is varied between 100 and 1000 hPa for the tropical profile.

5. HEIGHT DEPENDENT VARIATION OF RH

(a) *Experimental Design*

While section 4(b) highlights the strong negative correlation between TRH and clear-sky OLR, further experiments are necessary to quantify the effects of RH variation throughout the atmosphere. For this purpose, 5 additional experiments were undertaken whereby monthly-mean clear-sky OLR was calculated by the CLERA system using the 15 monthly-mean July fields from ERA. This differs from the reference version of CLERA used in Sec. 4 which accumulated the monthly-mean clear-sky OLR from values calculated every 6-hours. To assess the affect of RH variations on the clear-sky OLR, a control experiment was run using the 15 monthly-mean ERA fields. Perturbation experiments were subsequently run in which specific humidity was varied with ERA temperature to conserve ERA 15 year July mean RH at each grid point at specified sigma (σ) levels as defined in Table 1. The experiments are described as follows:

CTRh - Reference version of the CLERA simulation which used 6-hourly fields to construct monthly-mean irradiance and allowed RH to vary throughout the atmosphere.

CTRm - Control experiment in which RH was allowed to vary throughout the atmosphere. The only difference from CTRh is that monthly-mean input was used.

CONRH - RH was prescribed throughout the atmosphere by the 15 year July mean value.

UTRH - RH was allowed to vary only in the upper troposphere (see Table 1).

MTRH - RH was allowed to vary only in the middle troposphere (see Table 1).

LTRH - RH was allowed to vary only in the lower troposphere (see Table 1).

Note that the labels are used for convenience and are most appropriate for the tropical troposphere; in the extra-tropics, much of what is labelled as "upper troposphere" lies in the lower stratosphere.

TABLE 1. DESCRIPTION OF THE 5 EXPERIMENTS USING THE CLERA SIMULATION THAT CALCULATE JULY MONTHLY-MEAN CLEAR-SKY OLR FOR THE 15 YEARS OF THE ERA PERIOD USING MONTHLY-MEAN ERA PROFILES OF T AND q.

Experiment	**σ-levels**	**q(σ)**	**Approximate pressure levels between which RH varies**
CTRm	1 to 31	ERA	ALL
CONRH	1 to 31	$0.01\overline{RH(\sigma)}q_s(T(\sigma))$	NONE
UTRH	5 to 14	ERA	100 to 400 hPa
	5> σ >14	$0.01\overline{RH(\sigma)}q_s(T(\sigma))$	(Upper Troposphere)
MTRH	15 to 21	ERA	400 to 700 hPa
	15> σ >21	$0.01\overline{RH(\sigma)}q_s(T(\sigma))$	(Middle Troposphere)
LTRH	22 to 29	ERA	700 to 1000 hPa
	22> σ >29	$0.01\overline{RH(\sigma)}q_s(T(\sigma))$	(Lower Troposphere)

$q_s(T(\sigma))$ represents the saturation specific humidity as a function of the temperature at a given σ level. The 15 year July mean RH is denoted by $\overline{RH(\sigma)}$

Where RH is held constant, the specific humidity is calculated as:

$$q(\sigma) = 0.01\overline{RH(\sigma)}q_s(T(\sigma)), \tag{7}$$

where σ denotes sigma-level height coordinate, $\overline{RH(\sigma)}$ denotes the calculated 15 year July mean RH at a given level and $q_s(T(\sigma))$ denotes the saturation specific humidity for the ERA temperature of each level using an empirical form of the Clausius Clapeyron equation (from Liou 1980). At levels where RH is allowed to vary, ERA monthly-mean $q(\sigma)$ for the given year is used. Because of the non-linear dependence of clear-sky OLR on q and T, the global-mean clear-sky OLR from monthly-mean profiles (CTRm) is 1.8 Wm^{-2} less than the corresponding value for the reference version of CLERA which used 6 hourly calculations (CTRh) as shown in Table 2. Experiment CTRm was thus necessary to ensure consistency between perturbation and control experiments.

(*b*) *Global-mean clear-sky OLR variability*

The variability of the simulated clear-sky OLR can be characterised by its standard deviation (SD_{OLR}) for the 15 years. Table 2 shows that the global-mean standard deviation from CTRm is almost identical to that from CTRh, indicating that using monthly-mean input does not affect the interannual variability. However, the global mean standard deviation for CONRH, where RH is constant, is roughly half that of CTRm in which RH varies. Where RH is allowed to vary only in the upper, middle or lower troposphere, the standard deviation of clear-sky OLR is larger than for experiment CONRH showing that RH variations throughout the troposphere affect the global-mean clear-sky OLR variability. The OLR standard deviation for MTRH is the greatest and LTRH gives the lowest value. Therefore the order of importance for global variation in clear-sky OLR due to tropospheric RH variations is the middle, upper and then lower troposphere.

The correlation between *global-mean* clear-sky OLR and T_s is not significant at the 99.5 % level for experiment CTRh and CTRm. However, when RH is not allowed to vary (CONRH), a strong positive correlation of 0.85 is calculated with global-mean clear-sky OLR increasing at the rate of 2.3 $Wm^{-2}K^{-1}$. Thus changes in RH act to mask the dependence of clear-sky OLR on T_s in a global-mean sense. When all 180 global monthly mean clear-sky OLR values are used from CTRh, and the seasonal cycle is filtered out, a statistically significant correlation at the 99.9 % level is attained (r=0.49) with a $dOLR/dT_s$ of 2.1 $Wm^{-2}K^{-1}$. Thus changes in RH do not appear to greatly affect the dependence of clear-sky OLR on T_s, but merely the degree of linear correlation. The sensitivity of global-mean clear-sky OLR to T_s is similar to that inferred from climate models as discussed by Cess *et al.* (1990).

Figure 7 shows the global-mean clear-sky OLR plotted for each July with global-mean T_s for experiments CONRH (solid line) and CTRm (dotted line) and highlights the increase in correlation once the RH signal is removed. When considering years before 1985 the clear-sky OLR, for a given T_s, is greater than for years after 1985 for experiment CONRH. An additional run with the CLERA simulation was performed whereby the well mixed greenhouse gases are set at July 1979 levels while all other parameters are as defined in CTRm for July 1993. The global-mean clear-sky OLR difference due to changes in greenhouse gases over the 15 year period are calculated as 0.5 Wm^{-2} for the July 1993 profiles. This is enough to explain the apparent decrease of clear-sky OLR at a given T_s in Fig. 7. When clear-sky OLR is adjusted to account for the increasing concentrations of greenhouse gases, the correlation between global-mean clear-sky OLR and T_s increases for all experiments.

When only upper tropospheric RH is allowed to vary, in experiment UTRH, the sensitivity of global-mean clear-sky OLR to T_s is greater than for experiment CONRH (Table 2). Conversely, when only lower or middle tropospheric RH are allowed to vary $dOLR/dT_s$ is less than for experiment CONRH. This suggests that upper tropospheric RH variations counteract the thermodynamic water vapour feedback while RH variations in the lower and middle troposphere enhance the thermodynamic water vapour feedback. Using a t-test (Freund 1976), the values of $dOLR/dT_s$ for experiments CONRH and UTRH are not significantly different at the 95% confidence level. Therefore a longer data set is required to identify a negative feedback due to upper tropospheric RH. Thus, there is weak evidence that the negative water vapour feedback mechanism proposed by Lindzen (1990) may operate, but only in a small portion of the atmosphere. The remainder of the atmosphere appears to counteract the upper troposphere effect, causing the overall water vapour feedback to be strongly positive.

The OLR standard deviation is plotted for experiments CTRm in Fig. 8(a) and

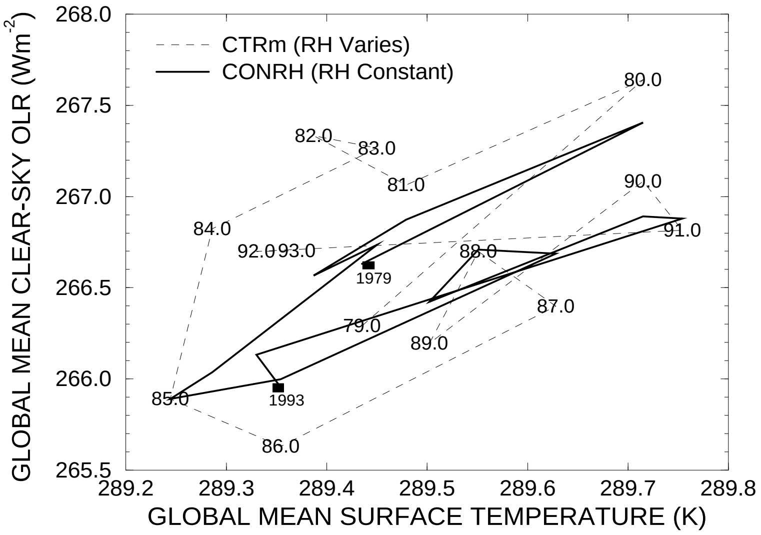

Figure 7. Global-mean clear-sky OLR (Wm^{-2}) for experiments CTRm (dashed line) and CONRH (solid line) plotted with global-mean T_s (K) for the 15 monthly-mean July's of the ERA period. Numbers within the frame denote year; individual years are annotated for CTRm and end points are noted for CONRH.

TABLE 2. July global-mean clear-sky OLR and SD_{OLR} for CLERA experiments. LSQF sensitivity of global-mean OLR to global mean T_s and its correlation coefficient is displayed in columns 4 and 5.

EXPERIMENT	OLR (Wm^{-2})	SD_{OLR} (Wm^{-2})	LSQF $\frac{dOLR}{dT_s}$ ($Wm^{-2}K^{-1}$)	LSQF r for $\overline{OLR} = a\overline{T_s} + b$
CTRh	268.5	3.0	1.38	0.41
CTRm	266.7	2.9	1.42	0.42
CONRH	266.5	1.5	2.28	0.85**
UTRH	266.6	1.9	2.46	0.81**
MTRH	266.6	2.1	1.66	0.60*
LTRH	266.5	1.7	1.93	0.76**

** denotes statistically significant correlation at greater than the 99.5 % confidence level. * denotes statistically significant correlation at greater than the 95 % confidence level.

CONRH in Fig. 8(b). The large SD_{OLR} of greater than 3 Wm^{-2} is present in both experiments for high latitude regions (most especially Antarctica) where the variation of clear-sky OLR is more dependent on changes in temperature than on changes in RH. The largest reduction in the SD_{OLR} occur over ocean regions within about 30° of the equator, most especially in the tropical central Pacific and the region north of the Arabian Sea. This reinforces the conclusions of section 4(b) that changes in RH control clear-sky OLR variation over middle and low latitudes while T_s appears to dominate the OLR variability over high latitude land regions.

(*c*) *Height dependent RH variation and clear-sky OLR*

Comparing standard deviations indicates the difference in variability over the 15 months between the experiments. However, a better measure of the fraction of clear-sky OLR variability due to changes in RH is to consider OLR anomaly differences between the control and perturbation experiments. Therefore the fraction of clear-sky OLR an-

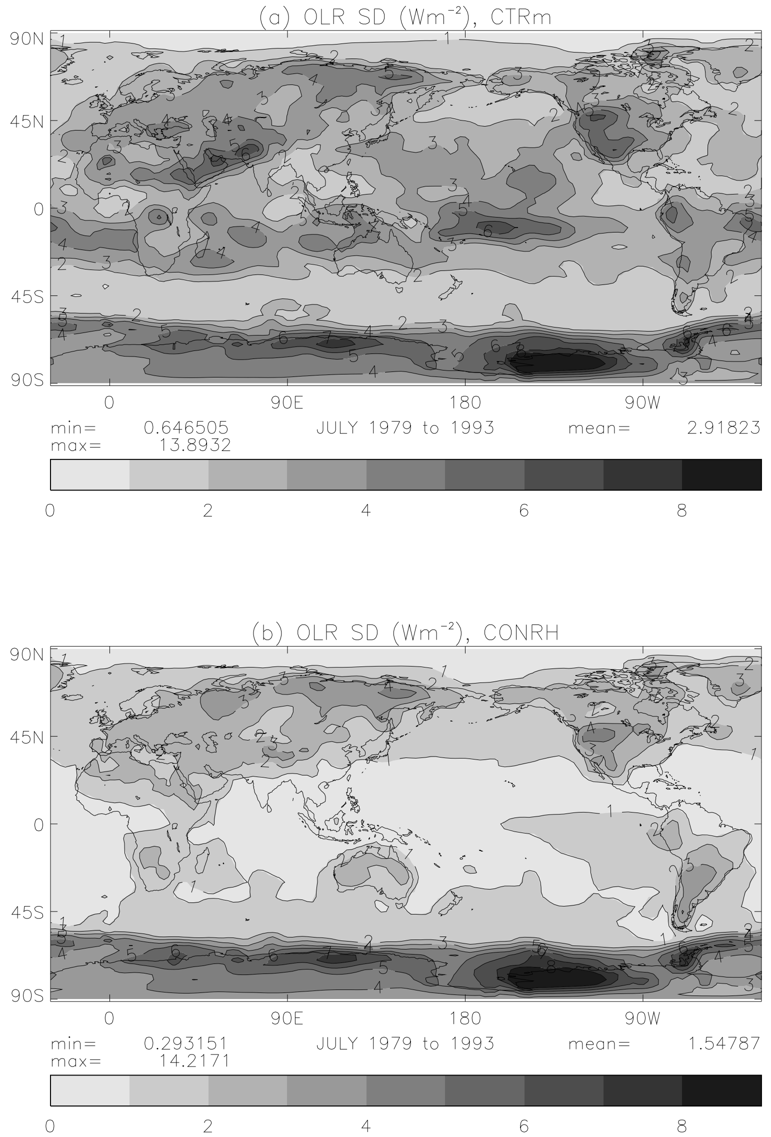

Figure 8. Clear sky OLR Standard deviation (Wm^{-2}) for July 1979 to 1993, plotted globally where (a) RH is allowed to vary (experiment CTRm) and (b) RH is held constant throughout the atmosphere (experiment CONRH). The contour interval is 1 Wm^{-2}.

omaly, ΔOLR, due to changes in RH may be calculated as follows for each grid point:

$$f_j = \frac{1}{N}\sum_{i=1}^{N}\left[\frac{(\Delta OLR_{i,j} - \Delta OLR_{i,CONRH})}{\Delta OLR_{i,CTRm}}\right], \tag{8}$$

where i denotes year, N is the number of years and j denotes experiments UTRH, MTRH, LTRH or CTRm. Only grid points where $(\Delta OLR_{i,CTRm})^2$ is greater than 4 $(Wm^{-2})^2$ are considered, to increase signal to noise ratio.

Figure 9 shows f averaged over 1 K T_s bins over ocean regions only for changes in RH throughout the troposphere (f_{RH}), and for changes in upper, middle and lower tropospheric RH calculated using Eq. (8). f_{RH} is about equal to the sum of f_{UTRH}, f_{MTRH} and f_{LTRH}. There is a rapid rise in f_{RH} with T_s, with RH explaining nearly all of the variation in clear-sky OLR at temperatures of about 300 K. For temperatures below about 290 K, much of this clear-sky OLR dependence on RH is due to middle tropospheric RH variations. At temperatures greater than about 290 K, changes in upper tropospheric RH become increasingly important as they do for changes in lower tropospheric RH at temperatures above 295 K. f_{UTRH} decreases at temperatures above about 300 K (mainly due to the tropical West Pacific regions). This may be a result of the smaller upper tropospheric RH variability for the most moist profiles. While the middle tropospheric RH appears to be the dominant control on clear-sky OLR away from high latitudes, the variations of RH *throughout* the troposphere contribute significantly to clear-sky OLR variability. When f is binned in land surface temperature intervals (not shown), values are generally lower than over the ocean. However, the importance of middle tropospheric RH and the rapid increase in f with T_s is still evident.

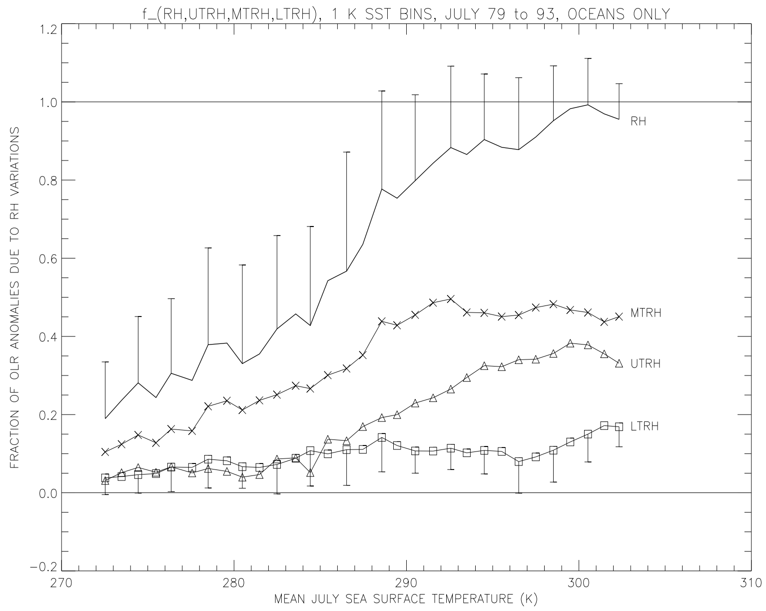

Figure 9. Fraction of clear-sky OLR anomalies due to changes in RH for $1K$ sea surface temperature bins calculated from experiments CTRm, CONRH, UTRH, MTRH and LTRH. Only grid points of clear sky OLR anomalies greater in magnitude than 2 Wm^{-2} are considered. Vertical bars denote one standard deviation about the mean value of f in the temperature bin and are plotted every alternate temperature bin for f_{RH} and f_{LTRH} only for clarity.

Figure 10(a) to (c) shows the global distribution of f for UTRH, MTRH and LTRH respectively. Experiment MTRH explains a significant amount of clear-sky OLR variability throughout much of the globe excluding Antarctica. This is especially so off the west coast of South America where middle tropospheric RH variations appear to exclusively control clear-sky OLR variations. Global-mean f_{MTRH} is 0.33 which implies that middle tropospheric RH variations account for, on average, about one third of the clear-sky OLR variation. f_{UTRH} is generally above 0.4 within about 40° of the equator and accounts for about 21% of the variation in clear-sky OLR variability. LTRH appears to contribute little to the clear-sky OLR variation (Fig. 10(c)). However, when averaged over the globe, about 11% of the clear-sky OLR variability is explained by changes in lower tropospheric RH. Thus the conclusions of section 5(b) are also supported by this analysis: (a) The order of importance of RH variations in influencing OLR variations is middle, upper and then lower tropospheric RH and, (b) RH throughout the atmosphere contributes significantly to changes in OLR from year to year.

(*d*) *The super-greenhouse effect*

Section 4(a) shows a SGE to act over tropical ocean regions for the interannual time-scale. This is explained in terms of the change in the convective regime due to the ENSO cycle that are associated with changes in T_s. When RH is held constant, as in experiment CONRH, there are no regions exhibiting a statistically significant SGE. This is consistent with Hallberg and Inamdar (1993) who show that thermodynamics alone is not enough to explain the SGE. Figure 11 shows the LSQF $dOLR/dT_s$ for experiments CTRm, CONRH, UTRH, MTRH and LTRH binned into 1 K intervals of T_s over the oceans. The binned sensitivity for experiment CONRH ranges from between about 1.0 $Wm^{-2}K^{-1}$ in the tropics to about 1.9 $Wm^{-2}K^{-1}$ elsewhere. A SGE is not apparent in any of the T_s bins for experiment CONRH while a SGE applies at sea surface temperatures above about 296 K for experiment CTRm albeit with a large scatter about the mean value for the bin. Allowing changes in RH for each layer results in a decreased $dOLR/dT_s$ compared to the CONRH experiment. The sum of $((dOLR/dT_s)_j - (dOLR/dT_s)_{CONRH})$, where j denotes experiments UTRH, MTRH and LTRH, is approximately equal to $(dOLR/dT_s)_{CTRm}$. A decrease in $dOLR/dT_s$ at high T_s for experiment CONRH shows that thermodynamics contributes to producing SGE situations because over the tropical oceans, clear-sky OLR is essentially decoupled from T_s. This is due to the large column moisture and therefore a small Tr term in Eq. (4). Allowing RH to vary only in the lower troposphere in experiment LTRH results in a similar $dOLR/dT_s$ to experiment CONRH. However for experiments MTRH and UTRH, $dOLR/dT_s$ is significantly lower at high sea surface temperatures. Thus it is mainly the changes in upper and middle tropospheric RH that cause SGE situations to occur. Similar conclusions have been drawn from other studies (e.g. Hallberg and Inamdar 1993).

6. DISCUSSION

A simulation of the Earth's clear-sky longwave radiation budget is used to examine the dependence of clear-sky OLR on surface and atmospheric temperature and relative humidity throughout the troposphere. Changes in T_s appear to dominate the clear-sky OLR variation at high latitudes, especially over the land regions, while over middle and low latitudes, changes in tropospheric RH appear to control clear-sky OLR variability. Globally, tropospheric RH explains a larger proportion of OLR variation over an interannual time-scale than over the seasonal cycle. This is because for a given change in TRH, variations in T_s are less over the interannual time-scale in all but the tropics.

A super-greenhouse effect (SGE; defined as negative $dOLR/dT_s$) is identified over both the seasonal and interannual time scales. When RH is held constant or only allowed to vary in the lower troposphere, no statistically significant SGE is produced. However, when upper or mid-tropospheric RH are allowed to vary, a SGE is identified over the interannual time-scale. The necessary change in RH is provided only when a change in

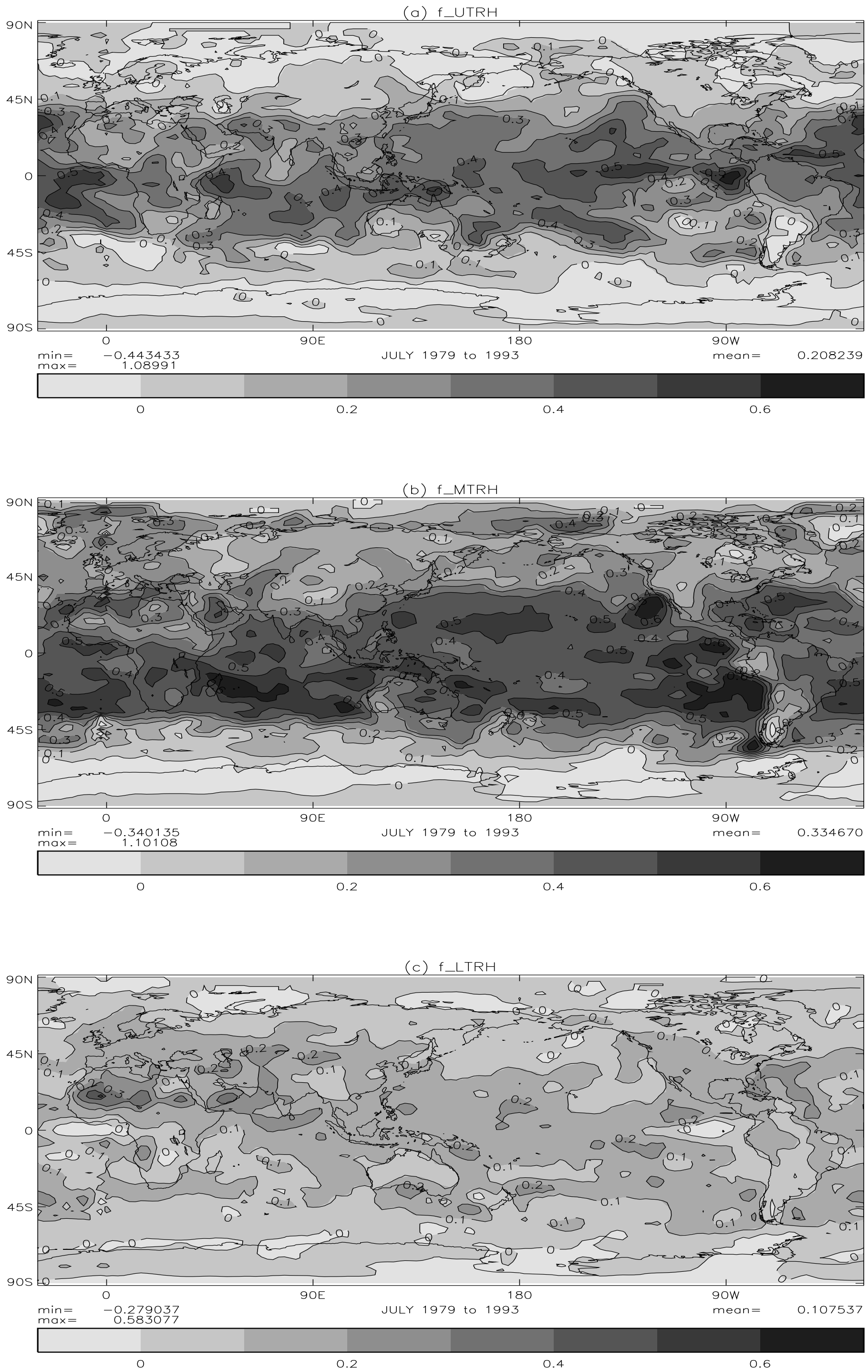

Figure 10. Fraction of clear-sky OLR anomalies due to changes in (a) upper, (b) middle and (c) lower tropospheric RH over the interannual time-scale for July. Only grid points where clear-sky OLR anomalies are greater in magnitude than 2 Wm^{-2} are considered. The contour interval is 0.1

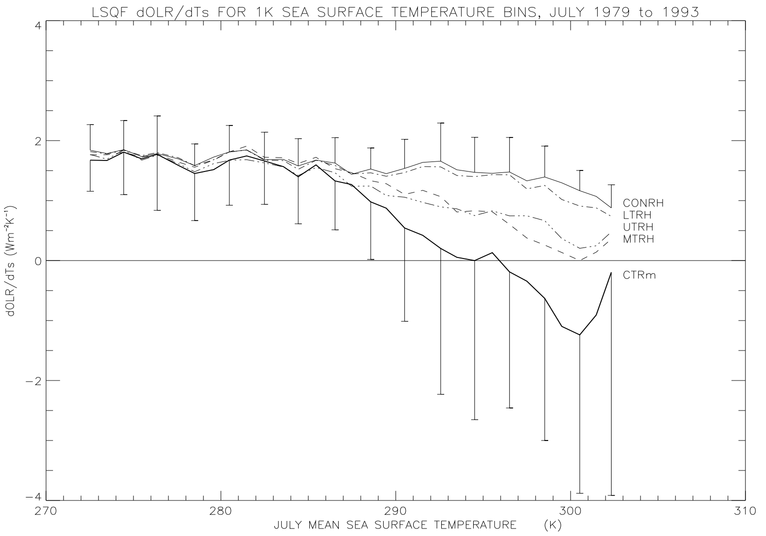

Figure 11. LSQF clear sky OLR sensitivity to changes in T_s over the oceans ($Wm^{-2}K^{-1}$) for July 1979 to 1993 calculated in 1 K T_s bins for experiment CTRm, CONRH, UTRH, MTRH and LTRH. Vertical bars denote one standard deviation about the mean value of $dOLR/dT_s$ and are plotted for experiments CONRH and CTRm only for reasons of clarity.

T_s is associated with a transition between strong and weak convection. This may only occur where ascent is imposed by the large scale circulation (Bony *et al.* 1997). Over the seasonal cycle, the shift in the Hadley circulation imposes such a transition in the tropics (although away from the equator) which corresponds with the regions exhibiting a SGE. On the interannual time-scale, the shift in the Walker circulation associated with ENSO is sufficient to alter the degree of convection in the tropical Pacific necessary to produce a SGE situation. Because the SGE constitutes an unstable radiative feedback to the surface (Inamdar and Ramanathan 1994), stabilising mechanisms such as short wave cloud radiative feedbacks, evaporative feedbacks and heat export to the extra tropics are required to prevent a local runaway greenhouse effect from operating (Pierrehumbert 1995).

The sensitivity of clear-sky OLR to TRH is most negative in regions of low TRH. This can be explained by the saturation of the water vapour absorption bands with increasing RH. In all but the most moist regions, clear-sky OLR is most sensitive to a given RH variation if that change is in the upper troposphere; Spencer and Braswell (1997) use this result to argue that upper tropospheric RH is highly important for climate change. However, because RH variations in the upper troposphere are generally associated with larger changes in RH at lower levels, the importance of upper tropospheric RH with regard to the clear-sky OLR may have been overstated. Because the ERA RH variations are greatest between about 600 and 800 hPa, the *middle* tropospheric RH contributes most to clear-sky OLR variability over the interannual time-scale. This supports the conclusions of previous studies (e.g. Clough *et al.* (1992); Sinha and Harries (1997)). By allowing RH to vary only in either the upper, middle or lower troposphere, it is shown that the middle troposphere (about 400 to 700 hPa) contributes about one third of the clear-sky OLR variability. The upper and lower troposphere contribute about 21% and 11% respectively. Therefore RH *throughout* the troposphere contributes significantly to clear-sky OLR variation. Changes in surface and atmospheric temperature account for the remaining 35% of the variability. There is weak evidence in support of a negative water vapour feedback, as suggested for example by Lindzen (1990), although this is only the case for the upper tropospheric RH variations; changes in RH at lower levels of the troposphere counteracts this effect, resulting in an overall positive water vapour feedback.

The results presented are relevant for interannual variation between Julys. Therefore conclusions are relevant for the interannual variability due to changes in the large scale circulation for this month. For example, changes in the Asian monsoonal circulation may be significant in dictating the variability of RH between Julys. The profound link between clouds and water vapour also render the present study incomplete with regard to the overall response of the climate system to a radiative forcing. For the experiments undertaken, changes in RH do not appear to significantly alter the relationship between global-mean clear-sky OLR and T_s, but merely decrease their linear correlation.

While information concerning the sensitivity of the Earth's radiation budget to observed changes in surface and atmospheric parameters yields valuable information as to the mechanisms acting in the climate system, climate model experiments are required to perform relevant climate sensitivity calculations. Unfortunately these studies themselves are limited by the potential inability of the model to parameterize accurately the moist convection so important in determining the water vapour and cloud feedbacks. Therefore it should be a pre-requisite that climate models should be able to reproduce the sensitivities and variability that are provided by observations and simulations such as the present study.

A major limitation of the CLERA simulation is the reliance on the numerical model calculations used in the ERA project. This is especially true of the upper troposphere and the dry descending oceanic 'deserts' where observational data are limited. Hence a large uncertainty is attached to ERA humidity and its variability in these regions (e.g. Spencer and Braswell 1997). The inference of the present study, that clear-sky OLR variability is dependent mainly on RH variations in the middle troposphere as opposed to the upper troposphere, is therefore dependent on the validation of ERA humidity variability, most especially in these dry regions of the atmosphere. The dry descending regions of low TRH are likely to be important with regard to the water vapour feedback. Not only is clear-sky OLR most sensitive to TRH variations in these regions but, unlike the moist tropics the cloud amount is small thus increasing the importance of clear-sky feedbacks. Also, the radiative cooling is a dominant diabatic term in the descending portions of the Hadley circulation. Thus in understanding the climate system and the water vapour feedback, attaining robust observations of humidity in these regions must be paramount. By testing the ability of climate models to capture the variability of moisture and the associated variability in the clear-sky greenhouse effect over sufficiently long time-scales confidence can be increased in prediction of future climate change.

Acknowledgement

We thank Mark Webb for help with the CLERA simulations. Richard Allan is funded by a NERC studentship (GT41/95/263) under CASE award with the Meteorological Office. Alison Pamment is funded by the Department of the Environment, Transport and the Regions under contract PECD 7/12/37. The referees and associate editor are thanked for their many helpful comments.

References

Bony, S., Lau, K. -M and Le Treut, H. 1995 Observational dependence of the water vapour and clear-sky greenhouse effect on sea surface temperatures: Comparison with climate warming experiments. *Clim. Dyn.*, **11**, 307–320

Bony, S., Lau, K. -M. and Sud, Y. C. 1997 Sea surface temperature and large-scale circulation influences on tropical greenhouse effect and cloud radiative forcing. *J. Clim.*, **10**, 2055–2077

Cess, R. D., *et al.* 1990 Intercomparison and interpretation of climate feedback processes in 19 atmospheric general circulation models *J. Geophys. Res.*, **95**, 16601–16615

Clough, S. A., Iacono, M. J. and Moncet, J. L. 1992 Line-by-line calculation of atmospheric fluxes and cooling rates: Application to water vapor. *J. Geophys. Res.*, **95**, 15761–15785

Cullen, M. J. 1993 The unified forecast/climate model. *Meteorol. Mag.*, **122**, 81-94

Edwards, J. M. and Slingo, A. 1996 Studies with a flexible new radiation code: I: Choosing a configuration for a large scale model. *Q. J. R. Meteorol. Soc.*, **122**, 689–719

Freund, J. E. 1976 *Statistics, A first course*, Prentice-Hall

Forster, P. M. de-F. and Shine, K. P. 1997 Radiative forcing and temperature trends from stratospheric ozone depletion. *J. Geophys. Res.*, **102**, 10841–10855

Hallberg, R. B. and Inamdar, A. K. 1993 Observations of seasonal variations in atmospheric greenhouse trapping and its enhancement at high sea surface temperature. *J. Clim.*, **6**, 920–931

Hartmann, D. L. and Michelsen, M. L. 1993 Large-scale effects on the regulation of tropical sea surface temperatures. *J. Clim.*, **6**, 2049–2062

IPCC 1990 *Climate change: The IPCC scientific assessment*, Eds. J. T. Houghton, G. J. Jenkins, J. J. Ephraums. Cambridge University Press

IPCC 1995 *Climate change 1994: Radiative forcing of climate change and an evaluation of the IPCC IS92 emissions scenarios*, Eds. J. T. Houghton *et al.* Cambridge University Press

Inamdar, A. K. and Ramanathan, V. 1994 Physics of greenhouse effect and convection in warm oceans. *J. Clim.*, **7**, 715–731

Lau, K. M., Ho, C. H. and Chou, M. D. 1996 Water vapor and cloud feedback over the tropical oceans: Can we use ENSO as a surrogate for climate change? *Geophys. Res. Lett.*, **23**, 2971–2974

Lindzen, R. S. 1990 Some coolness concerning global warming. *Bull. Am. Meteorol. Soc.*, **71**, 288–299

Liou K. -N. 1980 *An introduction to atmospheric radiation*, Academic Press

McClatchey R. A., Fenn R. A., Selby R. A., Voltz P. E. and Garing J. S. 1972 *Optical properties of the atmosphere*, Environmental Research paper no 411, Air Force Cambridge Research Labs., Bedford, MA, 107pp

McNally, A. P. and Vesperini, M. 1996 Variational analysis of humidity information from TOVS radiances. *Q. J. R. Meteorol. Soc.*, **122**, 1521-1544

Pierrehumbert, R. T. 1995 Thermostats, radiator fins and the local runaway greenhouse effect. *J. Atmos. Sci.*, **52**, 1784–1806

Ramanathan, V. and Collins, W. 1991 Thermodynamic regulation of ocean warming by cirrus clouds deduced from observations of the 1987 El Niño. *Nature*, **351**, 27–32

Raval, A. and Ramanathan, V. 1989 Observational determination of the greenhouse effect. *Nature*, **342**, 758–761

Raval, A., Oort, A. H. and Ramaswamy, V.	1994	Observed dependence of outgoing longwave radiation on sea surface temperature and moisture. *J. Clim.*, **7**, 807–821
Rind, D., Chiou, E. -W., Chu, W., Lasen, J., Oltmans, S., Lerner, J., McCormick, M. P. and McMaster, L.	1991	Positive water vapour feedback in climate models confirmed by satellite data. *Nature*, **349**, 500–503
Shine, K. P. and Sinha, A.	1991	Sensitivity of the Earth's Climate to height-dependent changes in water vapour mass mixing ratio. *Nature*, **354**, 382–384
Sinha, A. and Harries, J. E.	1997	The Earth's clear-sky radiation budget and water vapour absorption in the far infrared. *J. Clim.*, **10**, 1601–1614
Slingo, A. and Webb, M. J.	1992	Simulation of clear-sky outgoing longwave radiation over the oceans using operational analyses. *Q. J. R. Meteorol. Soc.*, **118**, 1117–1144
Slingo, A. and Webb, M. J.	1997	The spectral signature of global warming. *Q. J. R. Meteorol. Soc.*, **123**, 293–307
Slingo, A., Pamment, J. A. and Webb, M. J.	1998	A 15-year simulation of the clear-sky greenhouse effect using the ECMWF re-analyses: Fluxes and comparisons with ERBE. *J. Clim.*, **11**, 690–708
Soden, B. J. and Fu, R.	1995	A satellite analysis of deep convection, upper tropospheric humidity and the greenhouse effect. *J. Clim.*, **8**, 2333–2351
Soden, B. J.	1997	Variations in the tropical greenhouse effect during El Niño. *J. Clim.*, **10**, 1050–1055
Spencer, R. W. and Braswell, W. D.	1997	How dry is the tropical free troposphere? Implications for global warming theory. *Bull. Am. Meteorol. Soc.*, **78**, 1097–1106
Thompson, S. L. and Warren, S. G.	1982	Parameterization of outgoing infrared radiation derived from detailed radiative calculations. *J. Atmos. Sci.*, **39**, 2667-2680
Webb, M. J., Slingo, A. and Stephens, G. L.	1993	Seasonal variations of the clear sky greenhouse effect: the role of changes in atmospheric temperature and humidities. *Clim. Dyn.*, **9**, 117–129